30 Mar 2001, 4:30 pm - 6:30 pm

Numerical Study on 3-Dimensional Behavior of a Damaged Pile Foundation during the 1995 Hyogo-ken Nanbu Earthquake

Ryosuke Uzuoka
Earthquake Disaster Mitigation Research Center, EDM, RIKEN, Japan

Tetsuo Kubo
EDM and Nagoya Institute of Technology, Japan

Atsushi Yashima
Gifu University, Japan

Feng Zhang
Gifu University, Japan

NUMERICAL STUDY ON 3-DIMENSIONAL BEHAVIOR OF A DAMAGED PILE FOUNDATION DURING THE 1995 HYOGO-KEN NANBU EARTHQUAKE

Ryosuke Uzuoka
Earthquake Disaster Mitigation Research Center
EDM, RIKEN, Hyogo 673-0433, JAPAN
Atsushi Yashima
Gifu University
Gifu 501-1193, JAPAN

Tetsuo Kubo
EDM and Nagoya Institute of Technology
Nagoya 466-8555, JAPAN
Feng Zhang
Gifu University
Gifu 501-1193, JAPAN

ABSTRACT

The purpose of this study is to investigate the process of the damage to a pile foundation located on a reclaimed land during the 1995 Hyogo-ken Nanbu earthquake. A 3-dimensional effective stress analysis using a soil-pile-building model was conducted on a damaged building. The five stories building tilted in a northeast direction because of serious damages to the pile foundations. Sand boils and ground settlements due to liquefaction were observed around the building. The simulated results showed that the reclaimed fill layer liquefied during the earthquake, and horizontal displacements of several tens centimeters occurred at the ground surface. The spatial distributions of the damages to piles were discussed through the 3-dimensional simulation. Consequently, the simulated failure direction of piles was associated with the observed direction of building inclination. The simulation qualitatively reproduced that the most serious damage of PHC piles occurred at the northeast footing among the footings located on the building corners.

INTRODUCTION

Many buildings with pile foundation on reclaimed land were seriously damaged during the 1995 Hyogo-ken Nanbu earthquake. The damaged building tilted and /or settled, while no clear damage to superstructure was observed. The field investigations and analyses for some damaged buildings on reclaimed land were conducted to clarify the cause of damage [Fujii *et al.*, 1998]. The failure of pile foundation in reclaimed fill layer was observed, and it was suggested that large ground deformation due to liquefaction of reclaimed fill caused the serious damage.

Assuming that the ground deformation caused the damage of pile, the inclined direction of the building and pile was associated with the direction of ground surface displacement. However, the prediction of the inclined direction was out of scope, because past analyses for damage process were carried out by using 1-dimensional spring-mass model or 2-dimensional FE model. 3-dimensional analysis is needed to discuss the inclined direction of the building and the horizontal distribution of damage in the pile.

In this study, the process of the damage to a pile foundation located on a reclaimed land is simulated by 3-dimensional effective stress analysis using a soil-pile-building model. The five stories building which tilted in a northeast direction due to serious damage to the pile foundations was analyzed. Firstly, the vertical array records observed near the damaged building are simulated to verify the numerical model and clarify the direction of ground motion. Next, the spatial distribution of the damages to piles is discussed through the analysis of 3-dimensional soil-pile building system.

DAMAGED BUILDING

Figure 1 shows the location of the investigated building on Fukaehama man-made island at the east edge of Kobe City [Isemoto *et al.*, 1998]. The damaged building was about 350 m

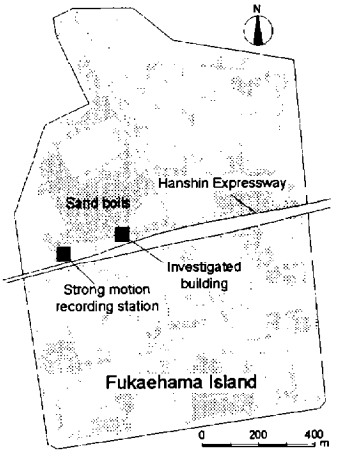

Fig. 1. Location of the investigated building [Reproduced from Isemoto et al., 1998]

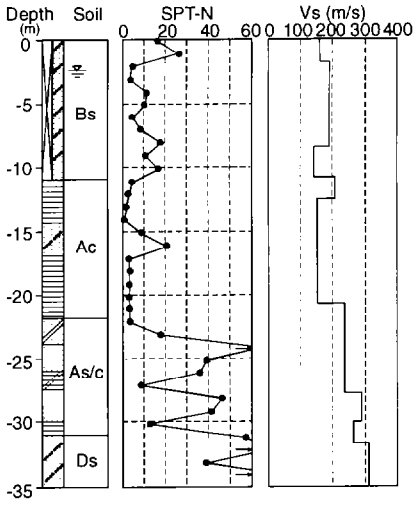

Fig. 2. Soil profile at the damaged site [Reproduced from Isemoto et al., 1998]

apart from the western quaywall. Sand and waters were ejected everywhere on the island after the earthquake [Hamada *et al.*, 1995]. Figure 2 shows the soil profile at the site where the damaged building located, with SPT-N values and shear wave velocities [Isemoto *et al.*, 1998]. The surface layer Bs is the reclaimed fill of well graded decomposed granite soils, called Masado, with averaged SPT-N value of about 10. The subsequent layers are the original seabed layer, Ac, of alluvial clay, and the alternate layers, As/c, of alluvial sand and clay. The water table was at the depth of about 2 m.

The damaged building was five stories building made of RC and PC structural members completed in 1988. Figure 3 shows the plan of the foundation. The each footing has two or three piles with the diameter of 500 mm or 600 mm. The RC footing girders are 400–650 mm wide and 1500 mm high. The pile length is 31 m, composed of three piles, one SC and two PHC piles as shown in Fig. 4. SC pile is a concrete pile reinforced by covered steel pipe, and PHC pile is a prestressed concrete pile made of high strength concrete. Type A has steel bars with a diameter of 7.1 mm. Figure 4 shows the investigated damage distribution of four piles, No.1-4 as shown in Fig. 3 [Isemoto *et al.*, 1998]. The cracks were indicated by the sonic integrity tests for No.1-3 piles. The large cracks and soil inside the pile were directly observed by the television camera for No.1 and No.4. The investigation showed that the serious failure of the piles was concentrated at the top of PHC piles with lower strength than SC piles. It was at the depth of about 10 m between the pile joints and the border of soil layers.

Figure 5 shows the horizontal displacement of surrounding ground and building [Isemoto *et al.*, 1998]. Measurements were conducted by comparing the aerial photographs before and after the earthquake. The building tilted in northeast direction, although the ground moved toward northwest direction. The inclination was 1/80 in the north direction, and 1/30 in the east direction. The settlement at the northeast footing of F1 was largest among F1-F3 as shown in Fig. 4. No clear damage to structural members of the superstructure, although the pile foundation was severely damaged.

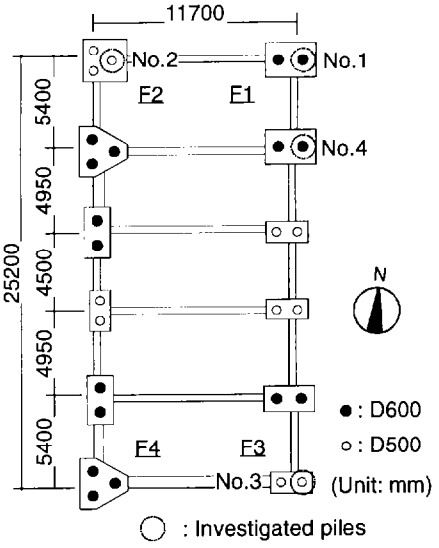

Fig. 3. Plan of foundation

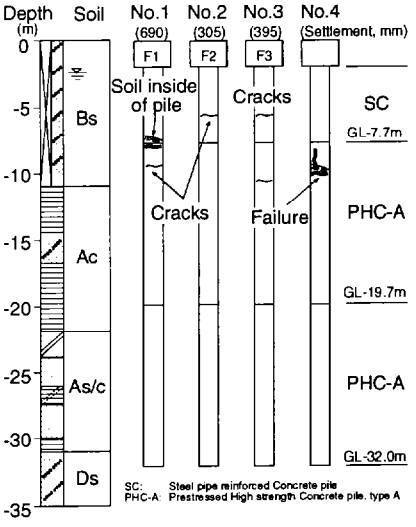

Fig. 4. Investigated damage distribution [Reproduced from Isemoto et al., 1998]

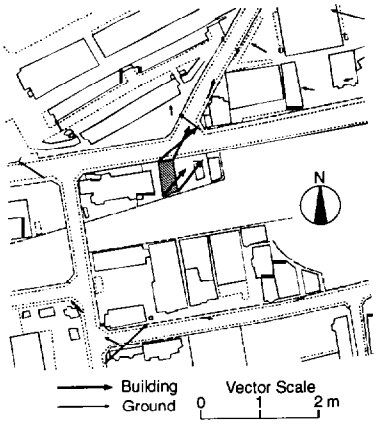

Fig. 5. Horizontal displacement of ground and building [Reproduced from Isemoto et al., 1998]

NUMERICAL METHOD

Governing Equations

In this study, the governing equations of for the coupling problems between soil skeleton and pore water were used based on a u-p formulation [Oka *et al.* 1994]. The finite element method (FEM) has been usually used for the spatial discretization of the governing equations. In this study, however, the finite element method (FEM) was used for the spatial discretization of the equilibrium equation, while the finite difference method (FDM) was used for the spatial discretization of the pore water pressure in the continuity equation. The accuracy of the proposed numerical method was verified by Oka *et al.* [1994] through a comparison of numerical results and analytical solutions for transient response of saturated porous solids. The governing equations are formulated by the following assumptions; 1) the infinitesimal strain, 2) the smooth distribution of porosity in the soil, 3) the small relative acceleration of the fluid phase to that of the solid phase compared with the acceleration of the solid phase, 4) incompressible grain particles in the soil. The equilibrium equation for the mixture is derived as follows:

$$\rho \ddot{u}_i^s = \sigma_{ij,j} + \rho b_i \tag{1}$$

where ρ is the overall density, $\ddot{u}_i^s$ is the acceleration of the solid, σ_{ij} is the total stress tensor and b_i is the body force. The continuity equation is derived as follows:

$$\rho^f \ddot{\varepsilon}_{ii}^s - p_{,ii} - \frac{\gamma_w}{k}\dot{\varepsilon}_{ii}^s + \frac{n\gamma_w}{kK^f}\dot{p} = 0 \tag{2}$$

where ρ^f is the density of the fluid, p is the pore water pressure, γ_w is the unit weight of the fluid, k is the coefficient of permeability, ε_{ii}^s is the volumetric strain of the solid, n is porosity and K^f is the bulk modulus of the fluid.

Constitutive Models

The constitutive equation used for sand is a cyclic elasto-plastic model [Oka *et al.*, 1999]. The constitutive equation is formulated by the following assumptions; 1) the infinitesimal strain, 2) the elasto-plastic theory, 3) the non-associated flow rule, 4) the concept of the overconsolidated boundary surface, 5) the non-linear kinematic hardening rule. The performance of the constitutive model was verified by Oka *et al.* [1999]. The model succeeded in reproducing the experimental results well under various stress conditions, such as isotropic and anisotropic consolidated conditions, with and without the initial shear stress conditions, principal stress axis rotation, etc.

The constitutive equation used for clay is a cyclic elasto-viscoplastic model [Oka, 1992]. The model is based on almost the same assumption of the elasto-plastic model for sand, except the flow rule of the model that is different from the model for sand. The model adopts the viscoplastic flow rule that can take the rate dependency of cohesive soil into account.

SIMULATION OF ARRAY RECORDS

The vertical array records observed near the damaged building are simulated to verify the numerical model and clarify the horizontal direction of ground motion. The recorded and computed orbits of the ground surface responses are compared.

Numerical Conditions

The vertical array strong motions during the earthquake were recorded at the observation station in Fig. 1 [Ministry of Construction, 1995]. The observation site was about 200 m apart from the damaged building. The obtained acceleration records in EW and NS direction at the depth of 33 m are shown in Fig. 6. It is noted that the number of cycles in EW direction was much fewer than that in NS direction for the amplitude of more than 0.25 m/s^2. These horizontal waves were used as input motions at the bottom of Ds layer. The vertical input was not considered in this study.

We applied the cyclic elasto-plastic model for sandy soil layers (Bs, As/c and Ds in Fig. 2), and the cyclic elasto-viscoplastic model for clay to the cohesive layers (Ac in Fig. 2). The soil profile in Fig. 2 was slightly modified to correspond to the in-situ condition at the observation site. The model parameters were determined by the in-situ tests and laboratory tests using undisturbed samples obtained from each soil layer. The physical property tests, undrained monotonic and cyclic triaxial tests were carried out after the

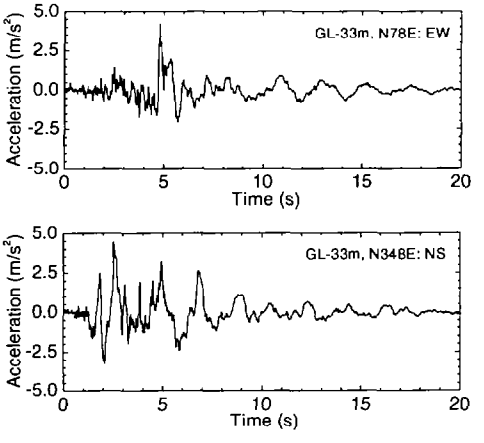

Fig. 6. Recorded acceleration at GL-33m [Ministry of Construction, 1995]

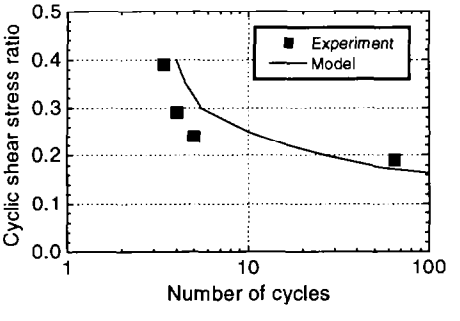

Fig. 7. Liquefaction strength

earthquake [Fujii *et al.*, 1998]. The liquefaction strength curves obtained by the laboratory tests and computed by the cyclic elasto-plastic model for Bs layer.

Numerical Results

Figure 8 shows the recorded and computed response accelerations for the direction of EW and NS at the ground surface. The computed accelerations agreed with the recorded ones, except that the slight phase difference between recorded and computed waves after about 5 seconds were shown. Figure 9 shows the excess pore water pressure ratio (E.P.W.P.R.) at the center depth of Bs layer. The E.P.W.P.R. means the ratio of excess pore water pressure for initial effective overburden pressure in this study. The initial liquefaction occurred at about 5 seconds, and the complete liquefaction occurred at about 8 seconds.

Figure 10 shows the recorded and computed particle orbits of horizontal acceleration, velocity and displacement at the ground surface. The computed velocity agreed with the recorded one regarding the maximum values and its directions. The computed predominant direction of displacement agreed with the recorded one, although the computed maximum displacement was about half as much as the recorded one. The computed liquefaction strength was slightly larger than the experimental one for a large shear stress ratio as shown in Fig. 7. Therefore, it is possible that the occurrence of complete liquefaction was later than the actual event. The error might cause the phase difference of acceleration after 5 seconds in Fig. 8, and the underestimation of horizontal displacement. Although the residual horizontal displacement in northwest direction was measured as shown in Fig.5, the recorded and computed residual displacement were not generated in northwest direction. Further investigation is needed for the direction of residual displacement.

SIMULATION OF DAMAGED BUILDING

The spatial distribution of the damage to piles is discussed through the analysis of 3-dimensional soil-pile building system. The observed and computed damage distributions to the piles are compared.

Numerical Conditions

Figure 11 shows the 3-dimensional FE model of soil-pile-building system. The soil layers were modeled by 8-node isoparametoric solid elements. We used the same constitutive models and parameters for each soil layer as the simulation of array records. The piles were modeled by beam elements with bilinear curvature-moment relations. No slip between the pile and soil was assumed. The crushing moment, which was defined as the compressive strain development of 0.25 % for concrete or the tensile strain development of 2.0 % for steel bar, was only considered. The crushing moment was calculated under the static axial load of 1100 kN for a pile. A few piles for a footing were modeled by a single equivalent pile, which had a simply summed moment of inertia and

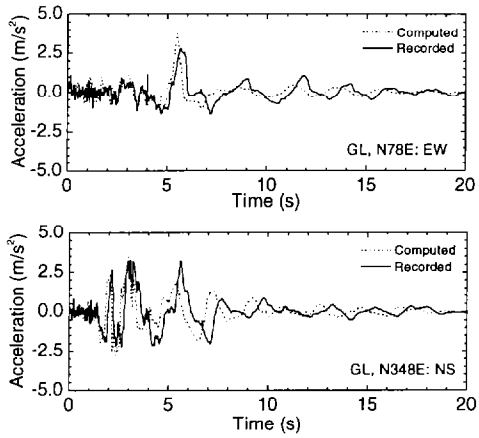

Fig. 8. Recorded and computed acceleration at GL [Recorded: Ministry of Construction, 1995]

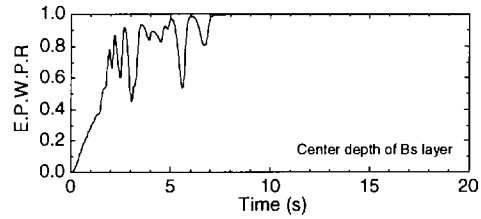

Fig. 9. Computed excess pore water pressure ratio

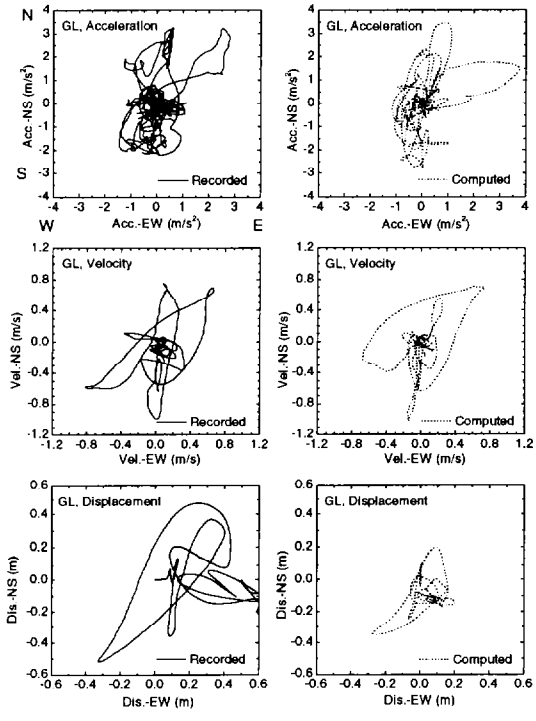

Fig. 10. Recorded and computed orbit [Recorded: Ministry of Construction, 1995]

sectional area for a footing. The properties of piles at the footing of only F1-F4 were summarized in Table 1. The building was modeled by linear beam elements for columns and girders, and linear shell elements for slabs and walls. The Young module of concrete for columns, girders and walls were set to 2.5E+7 kPa,

Table.1. Pile property

		F1-NE	F2-NW	F3-SE	F4-SW
Number of piles		2	3	2	3
Diameter	(mm)	600	500	500	600
Density	(t/m^3)	2.5	2.5	2.5	2.5
Young modulus	(kPa)	4.0E+07	4.0E+07	4.0E+07	4.0E+07
SC equivalent pile					
Sectional area	(m^2)	4.00E-01	4.56E-01	3.04E-01	6.01E-01
Moment of inertia	(m^4)	1.46E-02	1.15E-02	7.66E-03	2.19E-02
Crushing moment	(kNm)	1607	1735	1156	2411
Crushing curvature	(1/m)	2.75E-03	3.77E-03	3.77E-03	2.75E-03
PHC equivalent piles					
Sectional area	(m^2)	2.94E-01	3.23E-01	2.15E-01	4.42E-01
Moment of inertia	(m^4)	9.87E-03	7.39E-03	4.93E-03	1.48E-02
Crushing moment	(kNm)	980	1029	686	1470
Crushing curvature	(1/m)	2.48E-03	3.48E-03	3.48E-03	2.48E-03

and the slabs were assumed to be rigid. The additional mass for non-structural elements was distributed on the each slab.

The basement at the bottom of Ds layer was rigid, and all lateral boundaries were set to free. The horizontal plane of the water table was permeable, and all other boundaries were impermeable.

Numerical Results

Figure 12 shows the time history of horizontal displacement responses at the northeast footing of F1. The maximum displacement occurred at about 5.4 seconds in southwest direction, which coincided with the predominant direction of soil response as shown in Fig. 10. Other footings of F2-F4 showed similar displacement histories. Figure 13 shows the deformed configuration of FE model and the distribution of excess pore water pressure ratio on EW planes at the north and south edge of building at 5.4 seconds. Although the Bs layer liquefied partially, the shear deformation in Ac layer was predominant at this moment when the maximum acceleration was input.

Figure 14 and 15 shows the time histories and orbits respectively of moment and curvature of the top element of a PHC pile at the footing of F1. The output elements are located on the bottom element of Bs layer at the depth of 9.2 m. This moment is calculated for a single pile, and the crushing moment is 490 kNm. The PHC pile crushed firstly at about 3 seconds in NS direction and at about 5 seconds in EW direction. The maximum curvature in both directions occurred at 5.4 seconds, when the maximum horizontal displacement at the footing was generated. The curvature at the top element of a PHC pile occurred in northeast direction as shown in the deformation mode in Fig. 13. The residual curvature kept the northeast direction. Other piles showed similar tendencies for moment-curvature response. The failed direction of pile was associated with the observed direction of building inclination, although the deformation mode needed to be investigated regarding the occurrence of complete liquefaction in Bs layer.

Figure 16 shows the depth distributions of maximum curvature of piles at the footing of F1-F4. The curvature distributions in both

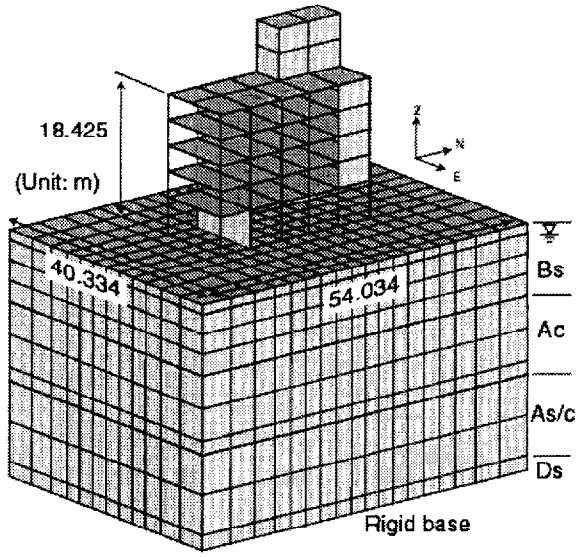

Fig. 11. FE model of soil-pile-building system

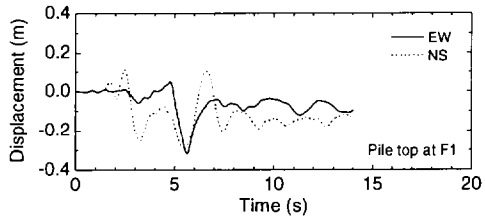

Fig. 12. Horizontal displacement at F1

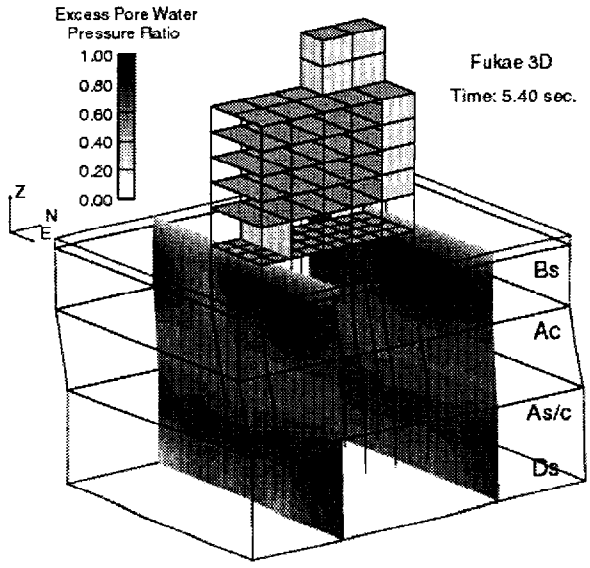

Fig. 13. Deformed configuration of FE model and distribution of excess pore water pressure ratio

directions had peak values at the border of soil layer. Moreover, the peak values on the top of SC piles were shown in NS direction only. These peak values were over the crushing curvatures as shown in Table 1. The simulated crushing at the bottom of Bs

layer agreed with the depth of actual serious damage to the piles, although the simulated damages were shown at the top of piles and at the bottom of Ac layer also. From the view of horizontal damage distribution, the maximum curvature of PHC piles at the footing of F1 became the largest at the bottom of Bs layer for EW and NS directions. The simulation qualitatively reproduced that the most serious damage of PHC piles occurred at the northeast footing of F1. The difference in damage of piles at among the four footings was due to the difference in horizontal distribution of the pile property and the ground deformation. The more detailed modeling of the piles, such as considering a moment-curvature relation depending on axial force and a nonlinear shear stress-strain relation, are needed for further investigation.

CONCLUSIONS

The process of the damage to a pile foundation located on a reclaimed land was simulated by 3-dimensional effective stress analysis using a soil-pile-building model, after the numerical model was verified based on the vertical array records near the damaged building. The simulated failure direction of piles was associated with the observed direction of building inclination. The simulation qualitatively reproduced that the most serious damage of PHC piles occurred at the northeast footing. We need further investigations for the occurrence time of complete liquefaction in reclaimed fill layer and more detailed damage distribution of the piles in the future.

ACKNOWLEDGEMENTS

The authors wish to thank Mr. Nishiraku of SHO-BOND Construction, Inc. and Mr. Koike of A & D Design Consultant, Inc. for providing the building data, and Mr. Isemoto of Toda Corporation for valuable suggestions about numerical analysis.

REFERENCES

Fujii, S., Isemoto, N., Satou, Y., Kaneko, O., Funahara, H., Arai, T. and Tokimatsu, K. [1998]. "Investigation and analysis of a pile foundation damaged by liquefaction during the 1995 Hyogoken-Nambu earthquake", Soils and Foundations, Special Issue on Geotechnical Aspects of the January 17 1995 Hyogoken-Nambu Earthquake, No.2, pp.179-192.

Hamada, M., Isoyama, R. and Wakamatsu, K. [1995]. *"The 1995 Hyogoken-Nanbu(Kobe) Earthquake, Liquefaction, Ground Displacement and Soil Condition in Hanshin Area"*, Association for Development of Earthquake Prediction, Tokyo, Japan.

Ministry of Construction [1995]. "Strong-Motion Acceleration Records from Public Works in Japan (No.21)", Technical Note of Public Works Research Institute, Vol. 64.

Isemoto, N., Kaneko, O., Sato, Y., Arai, T., Fujiwara, T. and Shirinashihara, S. [1998]. "Analytical studies on pile foundations damaged by soil liquefaction during the Hyogoken-Nanbu earthquake, Proceedings of the thirty-third Japan National Conference on Geotechnical Engineering, Yamaguchi, Japan, pp.801-802. (in Japanese)

Oka, F. [1992]. "A cyclic elasto-viscoplastic constitutive model for clay based on the non-linear hardening rule", Proc. 4th Int. Sym. on Numerical Models in Geomechanics, Swansea, pp105-114.

Oka, F., Yashima, A., Shibata, T., Kato, M., and Uzuoka, R. [1994]. "FEM-FDM coupled liquefaction analysis of a porous soil using an elasto-plastic model", Applied Scientific Research, 52, pp209-245.

Oka, F., Yashima, A., Tateishi, A., Taguchi, Y. and Yamashita, S. [1999]. "A cyclic elasto-plastic constitutive model for sand considering a plastic-strain dependence of the shear modulus", Geotechnique, No.5(49), pp.661-680.

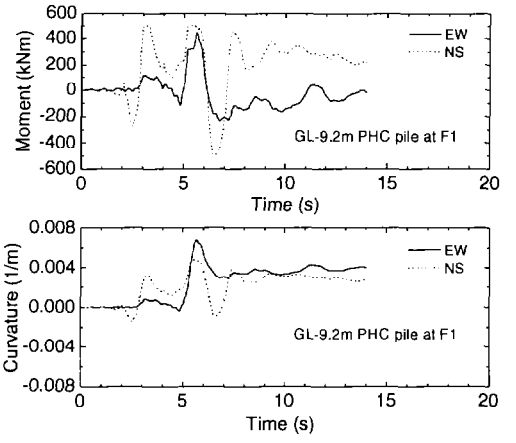

Fig. 14. Time history of moment and curvature

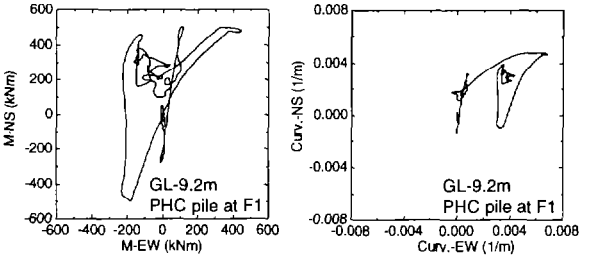

Fig. 15. Orbit of moment and curvature

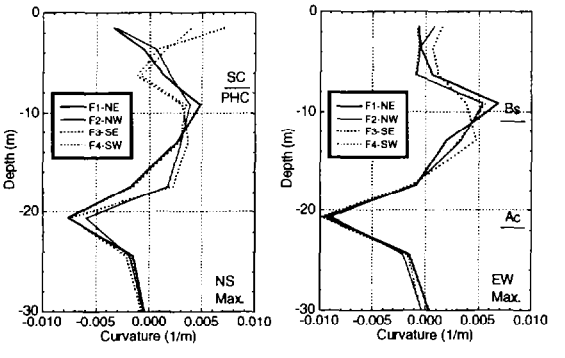

Fig. 16. Distribution of maximum curvature